

Measurement of the $1s2s\ ^1S_0-1s2p\ ^3P_1$ Intercombination Interval in Helium-like Silicon

M. Redshaw and E. G. Myers

Department of Physics, Florida State University, Tallahassee, Florida 32306-4350

(Received 31 August 2001; published 28 December 2001)

Using Doppler-tuned fast-beam laser spectroscopy the $1s2s\ ^1S_0-1s2p\ ^3P_1$ intercombination interval in $^{28}\text{Si}^{12+}$ has been measured to be $7230.5(2)\text{ cm}^{-1}$. The experiment made use of a single-frequency Nd:YAG($1.319\ \mu\text{m}$) laser and a high-finesse optical buildup cavity. The result provides a precision test of modern relativistic and QED atomic theory.

DOI: 10.1103/PhysRevLett.88.023002

PACS numbers: 31.30.Jv, 32.30.Bv

The low-lying levels of helium-like ions, see Fig. 1, provide important tests for relativistic atomic many-body theory — itself, arguably, an excellent laboratory for studying high-accuracy theoretical many-body techniques [1,2]. Although the underlying interaction (quantum electrodynamics) is well understood, the best way to formulate the problem to obtain accurate predictions remains the subject of much theoretical effort. At high- Z , S -matrix theory, e.g., see Refs. [3,4], provides a successful *ab initio* approach to the calculation of energy levels. However, at low and intermediate Z , because of the greater relative importance of electron correlation, methods starting with the nonrelativistic Schrödinger equation [5,6], or else a relativistic no-pair Dirac-Breit Hamiltonian [7–10], are more accurate in practice. Conventionally the results of these calculations are referred to as “structure,” while the remaining contributions, which can be derived only from field theory, are called “QED.”

In Ref. [7] Johnson *et al.* and in Ref. [8] Plante *et al.* used relativistic many-body perturbation theory (RMBPT) and an “all-orders”-RMBPT, respectively, while in Ref. [9] Chen *et al.* and in Ref. [10] Cheng *et al.* employed a related relativistic configuration-interaction technique (RCIT). These relativistic calculations obtain the structure energies up to order $(Z\alpha)^4$ a.u. (atomic units). References [7–9] employed QED corrections obtained by Drake [6], using earlier methods of Araki [11], Kabir and Salpeter [12], and Sucher [13]. Cheng *et al.* Ref. [10] obtained QED corrections using the scheme of Ref. [14]. Both these treatments of the explicit QED effects employ screening approximations and are incomplete at order $(Z\alpha)^4$ a.u. However, as discussed in [1,3], RMBPT and S -matrix theory are closely related, and improved calculations of the required QED corrections, derived from S -matrix theory, are feasible. As for the Lamb shift in hydrogen-like ions, the explicit QED effects, such as those involving the electron self-energy and vacuum polarization, are largest for s states.

However, as noted in Refs. [8–10], at least for $Z > 10$, the present generation of relativistic calculations predict the results of x-ray spectroscopy, e.g., see [15,16], and also of ultraviolet spectroscopy of the intrashell $1s2p\ ^3P-1s2s\ ^3S$ transitions, e.g., see [17],

quite satisfactorily at current experimental precision. A discrepancy, at the two-standard deviation level, was, however, observed in Ar^{16+} [18]. Laser spectroscopy of the $1s2s\ ^3S-1s2p\ ^3P$ transitions in Li^+ , e.g., [19], Be^{2+} [20], and B^{3+} [21] has achieved much higher precision. But here Z is too low for current RMBPT methods to obtain sufficient accuracy compared to the smallness of the QED corrections, and the techniques of Drake and coworkers are more appropriate [5,6]. Extension of laser spectroscopy of these transitions to higher Z is difficult because they move further into the ultraviolet. Laser spectroscopy of helium-like ions has been reviewed in [22]. As shown in Ref. [23], a path for extending the precision of laser techniques to higher Z helium-like ions is via the $1s2s\ ^1S_0 - 1s2p\ ^3P_1$ intercombination transition, which lies in the laser-accessible infrared up to $Z = 40$. In Ref. [24] this interval was measured in N^{5+} to 3×10^{-9} a.u., or 5×10^{-4} in units of $(Z\alpha)^4$ a.u., far more precise than current published theory. However, the convergence of the relativistic perturbation methods is still relatively poor at $Z = 7$ and better agreement was obtained with the “Unified method” [6]. Here we describe a measurement of the $1s2s\ ^1S_0 - 1s2p\ ^3P_1$ intercombination interval at substantially higher Z , where correlation effects, compared to the interesting QED effects, are significantly smaller. The experimental sensitivity, better than 10^{-6} a.u., or $8 \times 10^{-3}(Z\alpha)^4$ a.u.,

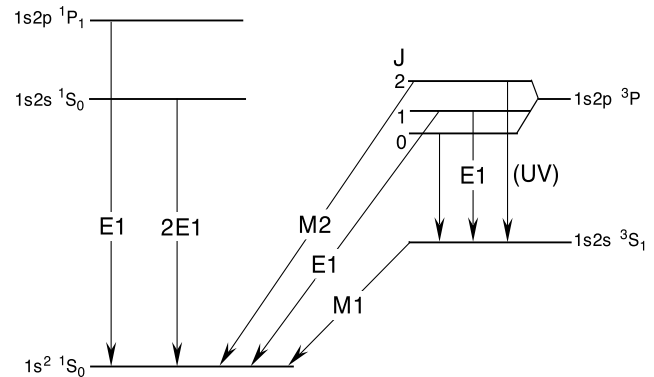


FIG. 1. Schematic of the $n = 2$ energy levels of helium-like ions showing the multiplicities of the principal radiative decay modes.

tests the total QED contribution to better than 0.05%, and is an order of magnitude higher than that obtained from ultraviolet spectroscopy at similar Z . Our result clearly differentiates between the various current theories and provides motivation for further theoretical work.

The main difficulty in extending spectroscopy of the $n = 2$ intercombination interval to higher Z is that the laser induced transition probability, for a given laser intensity, falls as $\sim Z^{-6}$. The rapidly increasing radiative decays of the various levels shown in Fig. 1 cause signal-to-background ratios to fall even faster [22]. Because continuous-wave techniques are more compatible with high ultimate precision, and for economy, we chose to work cw and increase the laser power at the interaction region using a high-finesse build-up cavity (BUC). In Si^{12+} the wavelength of the $1s2s\ ^1S_0 - 1s2p\ ^3P_1$ interval is approximately $1.383\ \mu\text{m}$, making a convenient match with the $1.319\ \mu\text{m}$ (second strongest) laser line of Nd^{3+} :YAG, allowing for the $\sim 5\%$ Doppler shift with a fast ion beam at $1\ \text{MeV}/u$.

Beams of $^{28}\text{Si}^{5+}$ and $^{28}\text{Si}^{6+}$ ions were obtained from the Florida State University FN tandem accelerator at energies of approximately 29.1 MeV. The ions were analyzed in a 90° bending magnet, collimated and focused to a beam diameter of approximately 1 mm, with currents of 10 or 1 particle-nA (for $5+$, $6+$, respectively), and then passed through a 10 or a $4\ \mu\text{g cm}^{-2}$ (nominal thickness) carbon foil. This yielded a Si^{12+} fraction of up to 7.5% [25] of which of the order of 1% were formed in the metastable $1s2s\ ^1S_0$ level, mean lifetime 11.5 ns [26]. The Si^{12+} charge state was then deflected 5° horizontally by a dipole magnet, bringing it colinear with the standing wave inside the BUC. At a distance 6.5 cm down-beam from the magnet pole face, and 25 cm from the foil, the ions passed through the waist of the laser beam in the BUC, and 1.9 cm above the $2\ \text{cm} \times 3\ \text{cm}$ window of a proportional counter. This was optimized for detection of 1.85 keV $1s2p\ ^3P_1 - 1s^2\ ^1S_0$ X rays, and to suppress detection of the two-photon continuum from the decay of $1s2s\ ^1S_0$, by operating with Ar/CH_4 (P-10) at atmospheric pressure and using a double window consisting of $1.5\ \mu\text{m}$ Mylar and $1\ \mu\text{m}$ polypropylene. The background X-ray count rate was 2.2 kHz per particle-nA for the thin foil and 4.2 kHz per particle-nA for the thick foil, due mainly to the 17% $M2$ x-ray decay branch of $1s2p\ ^3P_2$ level, with mean lifetime 4.34 ns [27]. When the copropagating laser beam was doppler shifted into resonance with the $1s2s\ ^1S_0 - 1s2p\ ^3P_1$ transition, population was transferred to the $1s2p\ ^3P_1$ level, mean lifetime 6.36 ps [27], at an estimated rate of $7 \times 10^3\ \text{s}^{-1}$ per W mm^{-2} per ion. The signal was the increase in x-ray yield due to the subsequent decay of $1s2p\ ^3P_1$ to the ground state. The resonance was scanned by varying the beam velocity, hence varying the Doppler shift, by scanning the field in the 90° magnet [24]. The laser induced signal was detected by modulating the power in the BUC at 50 Hz.

The design of the BUC followed the work of Ref. [28] and used 1 m radius-of-curvature superpolished mirrors [29], spaced 90 cm apart using invar rods inside the vacuum chamber. The cavity was excited using a laser-diode-pumped monolithic Nd:YAG laser [30] which, during the experiment, produced an output of 210 mW. The laser was locked to one of the approximately 2 kHz FWHM resonances of the passively stabilized cavity using the Pound-Drever-Hall scheme [31] with electro-optic modulation at 4 MHz. Because of the inherent frequency stability of this laser, and its convenient piezo (fast) and thermal (slow) tuning capabilities, a simplified servo-amplifier based on the work of De Riva *et al.* [32] sufficed. The chamber was evacuated to $<10^{-6}$ mbar using a “magnetically levitated” turbo-molecular pump and a LN_2 cold trap. For the final measurements we used the $4\ \mu\text{g cm}^{-2}$ thick foil. The rate of foil thickening and degradation under ion beam bombardment was reduced by scanning it across the ion beam and partially surrounding it with its own LN_2 cold trap. The circulating intracavity power in the BUC was estimated from the transmitted power to be 2.4 kW. The laser wave number remained stable to within $\pm 0.01\ \text{cm}^{-1}$ throughout the experiment, and was measured to the same absolute accuracy using a commercial wave meter [33].

A search in beam energy over the region predicted by Ref. [8] revealed a resonance of the expected height and width. A subsequent search, corresponding to the wave number region 7250.3 to $7268.5\ \text{cm}^{-1}$, which covers the predictions of Refs. [6,10], showed no resonance within statistics. The scans used for our final measurements are shown in Fig. 2. The peak signal height is consistent with the estimated transition probability. The observed resonance width, equivalent to $1.03 \pm 0.3\ \text{cm}^{-1}$ FWHM, is consistent with the (Lorentzian) natural width of $0.834\ \text{cm}^{-1}$, the estimated transition probability, which leads to power broadening (due to depopulation of $1s2s\ ^1S_0$) of approximately 10%, and a Gaussian contribution of $0.3\ \text{cm}^{-1}$, due to an estimated beam energy spread after the foil of 50 keV FWHM [34–36].

The statistical precision of the data in Fig. 2 is consistent with obtaining the wave number of the intercombination transition to 1 ppm. In the present experiment the precision is mainly limited by the uncertainty in the beam velocity, due to uncertainty in the magnet calibration and in the energy lost in the foil. To calibrate the 90° magnet we made use of the well known $^{19}\text{F}(p, \alpha\gamma)^{16}\text{O}$ nuclear resonance occurring at a proton energy of 872.11(20) keV [37]. We used $^{19}\text{F}^{3+}$ and $^{19}\text{F}^{4+}$ ions as the projectiles, a low pressure (0.01 mbar) CH_4 gas target, and BiGeO_4 scintillation detectors for gamma-ray detection. This produced symmetric Lorentzian resonances at fields near 9740 and 7307 G, respectively. In our arrangement the gas target was located up-beam of the interaction chamber. To measure the foil thickness we used the same nuclear reaction, but for the target we used the thin hydrogen

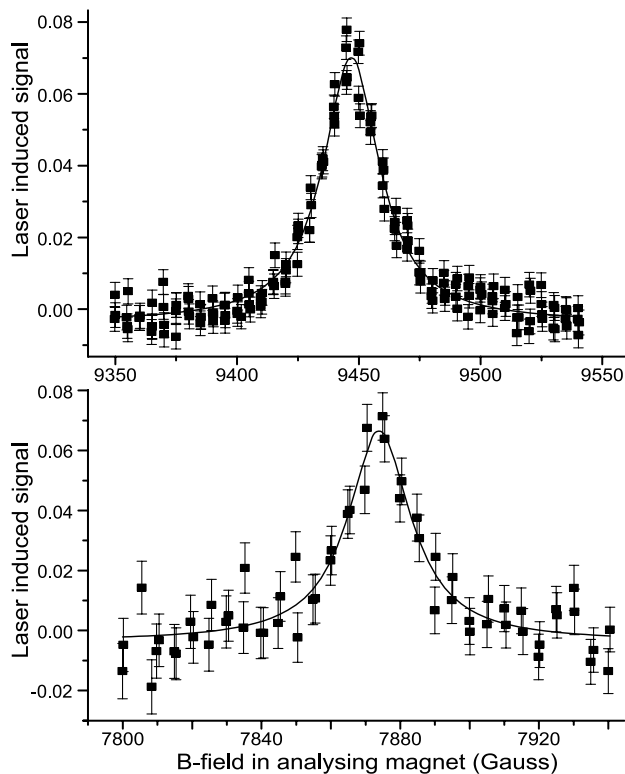


FIG. 2. Doppler tuned resonances of the $^{28}\text{Si}^{12+} 1s2s \ ^1S_0 - 1s2p \ ^3P_1$ intercombination transition, with Si^{5+} (upper), and Si^{6+} (lower) ions incident on a nominally $4 \mu\text{g cm}^{-2}$ carbon foil. The horizontal axis is the magnetic field in the analysing magnet used to determine the beam velocity. The vertical axis is the fractional increase in count rate due to the laser. The solid lines are least-squares fits with Lorentzians.

containing layer on our beam stop (which was covered with a thick gold foil), which typically forms under ion bombardment in non-ultrahigh vacuum conditions. This type of target has been characterized by Evers *et al.* [38] and was satisfactorily used for accelerator calibration. However, because of uncertainty in the actual distribution of protons within the surface layer, we used it only to measure the energy loss of the ^{19}F ions in the carbon foil, to give the foil thickness, and not for absolute energy calibration. This was done before and after the final Si runs, and revealed no significant foil thickening during those measurements. Using the 90° magnet fields corresponding to the laser and gas target nuclear resonances, plus the measurement of ^{19}F energy loss in the foil, we derived the values of $\beta\gamma$ corresponding to the Si^{12+} laser resonances, see Eq. (1) of Ref. [35]. Hence, using the relativistic Doppler formula and the measured laser wave number, we derived the $1s2s \ ^1S_0 - 1s2p \ ^3P_1$ wave number.

The error budget is shown in Table I. The statistical error is based on the fits to the Si^{12+} resonances and the corresponding fits to the gas target resonances (including the error in extrapolation to zero target thickness) used in the calibration. [The $\text{Si}^{5+,12+}$ measurement calibrated against F^{3+} gave $7230.40(4) \text{ cm}^{-1}$, compared to

$7230.37(5) \text{ cm}^{-1}$ for $\text{Si}^{6+,12+}$ against F^{4+} , statistical errors only.] The uncertainty due to the nuclear resonance energy, which we took as $16.448(10) \text{ MeV}$, takes account of the uncertainty in the proton energy [37] and in the conversion to inverse kinematics [39]. The day-to-day reproducibility of the absolute energy calibration of the 90° magnet was determined from the reproducibility of the nuclear resonance energies. The differential magnet calibration, $d(m\beta\gamma/q)/dB$, over the range of interest, was obtained from the $^{19}\text{F}^{3+}$ and $^{19}\text{F}^{4+}$ gas target resonances. The result agreed with the usual “one-point and zero” calibrations through the individual measurements to within 0.13%. Our foil thickness measurement, $4.7(9) \mu\text{g cm}^{-2}$, allows for the statistical and systematic fitting uncertainty of our solid target data and also the 5% quoted uncertainty in the stopping power of carbon for ^{19}F ions [40]. In converting this into the momentum loss of the silicon ions we allowed for the possible nonequilibrium increase in stopping power of the thin foil, for ions leaving in the $\text{Si}^{12+} 1s2s \ ^1S_0$ state compared to the rms charge state of 10.2 [25]. This was done by increasing the stopping power of Ref. [40] by $16 \pm 16\%$ [35,41]. The uncertainties due to noncolinearity in the laser-ion beam alignment ($<4 \text{ mrad}$), and laser and ion beam divergence, are negligible here. Including the correction for nonequilibrium stopping power, and combining the errors in Table I in quadrature, we obtain $7230.5(2) \text{ cm}^{-1}$ (1σ) as our final result. A similar analysis for the data with the nominally $10 \mu\text{g cm}^{-2}$ foil, which was not scanned, and which was used without the LN_2 traps in the chamber, and where the average BUC power was a factor of 8 lower, yielded $7230.6(3) \text{ cm}^{-1}$.

Our result and the results of the various calculations are shown in Table II. The best agreement is with the all-orders-RMBPT results of Plante *et al.* [8] who used the QED corrections of Drake [6]. The remaining discrepancy, equivalent to $0.025(8) (Z\alpha)^4 \text{ a.u.}$, is a factor of 6 smaller (scaled as Z^4) than the two standard-deviation discrepancy observed in UV spectroscopy of the $1s2s \ ^3S - 1s2p \ ^3P_{0,2}$ intervals of helium-like argon [18]. The RCIT calculations of Cheng *et al.* [10] are in strong disagreement, apparently due mainly to their QED corrections. Agreement is improved if these are replaced with

TABLE I. Contributions to the error in the measurement in parts-per-million.

Statistical (fitting)	5
Energy of the nuclear resonance	15
Absolute magnet calibration	15
Differential magnet calibration	4
Foil thickness	10
Silicon stopping power	11
Ion and laser beam overlap	<3
Intersection angle	0.4
Laser wave number	1.4
Total	27

TABLE II. The experimental result for the $^{28}\text{Si}^{12+} 1s2s \ ^1S_0 - 1s2p \ ^3P_1$ intercombination interval compared with recent theory. Units are cm^{-1} .

This experiment	7230.5(2)
Plante, Johnson, and Sapirstein [8]	7231.1
Cheng, Chen, Johnson, and Sapirstein [10]	7264.7
Drake [6]	7251.8
Cheng <i>et al.</i> [10], Drake [6] (QED)	7228.9

those of Drake, as shown in the last line of Table II [42]. Further work in both the structure and QED parts of the theory is indicated. The precision of the experiment can be improved, perhaps by an order of magnitude, by employing a co- and counterpropagating beam technique [24,34], or by precision time-of-flight measurement of the beam velocity.

We thank J. D. Silver and members of the Oxford EBIT group for the loan of the wave meter and for discussions concerning build-up cavities, S. L. Tabor and B. Roeder for assistance with gamma-ray spectroscopy and K. W. Kemper for his support and encouragement. The important contributions of J. K. Thompson, R. Harry, J.-S. Cho, J. Parnell, R. K. Nadaskay, and of other students and staff of the Florida State University Superconducting Accelerator Laboratory are gratefully acknowledged. This work was partially supported by NSF Grants No. PHY-9970991 and No. PHY-0098142, NATO CRG-960003, and the state of Florida.

[1] J. Sapirstein, *Rev. Mod. Phys.* **70**, 55 (1998).
 [2] I. Lindgren, *Int. J. Quantum Chem.* **57**, 683 (1996).
 [3] P. J. Mohr and J. Sapirstein, *Phys. Rev. A* **62**, 052501 (2000).
 [4] H. Persson, S. Salomonson, P. Sunnergren, and I. Lindgren, *Phys. Rev. Lett.* **76**, 204 (1996).
 [5] G. W. F. Drake, in *The Hydrogen Atom: Precision Physics of Simple Atomic Systems*, edited by S. G. Karshenboim *et al.* (Springer, New York, 2001), p. 57.
 [6] G. W. F. Drake, *Can. J. Phys.* **66**, 586 (1988).
 [7] W. R. Johnson and J. Sapirstein, *Phys. Rev. A* **46**, R2197 (1992).
 [8] D. R. Plante, W. R. Johnson, and J. Sapirstein, *Phys. Rev. A* **49**, 3519 (1994).
 [9] M. H. Chen, K. T. Cheng, and W. R. Johnson, *Phys. Rev. A* **47**, 3692 (1993).
 [10] K. T. Cheng, M. H. Chen, W. R. Johnson, and J. Sapirstein, *Phys. Rev. A* **50**, 247 (1994).
 [11] H. Araki, *Prog. Theor. Phys.* **17**, 619 (1957).
 [12] P. K. Kabir and E. E. Salpeter, *Phys. Rev.* **108**, 1256 (1957).
 [13] J. Sucher, *Phys. Rev.* **109**, 1010 (1958).
 [14] K. T. Cheng, W. R. Johnson, and J. Sapirstein, *Phys. Rev. A* **47**, 1817 (1993).

[15] R. E. Marrs, S. R. Elliott, and Th. Stöhlker, *Phys. Rev. A* **52**, 3577 (1995).
 [16] C. T. Chantler, D. Paterson, L. T. Hudson, F. G. Serpa, J. D. Gillaspay, and E. Takács, *Phys. Rev. A* **62**, 042501 (2000).
 [17] D. J. H. Howie, J. D. Silver, and E. G. Myers, *J. Phys. B* **29**, 927 (1996).
 [18] K. W. Kukla *et al.*, *Phys. Rev. A* **51**, 1905 (1995).
 [19] E. Riis, A. G. Sinclair, O. Poulsen, G. W. F. Drake, W. R. C. Rowley, and A. P. Levick, *Phys. Rev. A* **49**, 207 (1994).
 [20] T. J. Scholl, R. Cameron, S. D. Rosner, L. Zhang, R. A. Holt, C. J. Sansonetti, and J. D. Gillaspay, *Phys. Rev. Lett.* **71**, 2188 (1993).
 [21] T. P. Dinneen, N. Berrah-Mansour, H. G. Berry, L. Young, and R. C. Pardo, *Phys. Rev. Lett.* **66**, 2859 (1991).
 [22] E. G. Myers, in *The Hydrogen Atom: Precision Physics of Simple Atomic Systems*, edited by S. G. Karshenboim *et al.* (Springer, New York, 2001), p. 179.
 [23] E. G. Myers, J. K. Thompson, E. P. Gavathas, N. R. Claussen, J. D. Silver, and D. J. H. Howie, *Phys. Rev. Lett.* **75**, 3637 (1995).
 [24] J. K. Thompson, D. J. H. Howie, and E. G. Myers, *Phys. Rev. A* **57**, 180 (1998).
 [25] K. Shima, N. Kuno, M. Yamanouchi, and H. Tawara, *At. Data Nucl. Data Tables* **51**, 173 (1992).
 [26] A. Derevianko and W. R. Johnson, *Phys. Rev. A* **56**, 1288 (1997).
 [27] W. R. Johnson, D. R. Plante, and J. Sapirstein, *Adv. At. Mol. Opt. Phys.* **35**, 255 (1995).
 [28] M. S. Fee, S. Chu, and A. P. Mills, Jr., R. J. Chichester, D. M. Zuckerman, E. D. Shaw, and K. Danzmann, *Phys. Rev. A* **48**, 192 (1993).
 [29] Supplied by Research Electro-Optics, Inc.
 [30] Lightwave Electronics, Inc., Model No. 126-1319-350.
 [31] R. W. P. Drever, J. L. Hall, F. V. Kowalski, J. Hough, G. M. Ford, A. J. Munley, and H. Ward, *Appl. Phys. B* **31**, 97 (1983).
 [32] A. M. De Riva *et al.*, *Rev. Sci. Instrum.* **67**, 2680 (1996).
 [33] Burleigh Inc., Model No. WA-1000.
 [34] E. G. Myers, H. S. Margolis, J. K. Thompson, M. A. Farmer, J. D. Silver, and M. R. Tarbutt, *Phys. Rev. Lett.* **82**, 4200 (1999).
 [35] E. G. Myers and M. R. Tarbutt, *Phys. Rev. A* **61**, 010501(R) (2000).
 [36] B. Effen, D. Hahn, D. Hilscher, and G. Wüstefeld, *Nucl. Instrum. Methods* **129**, 219 (1975).
 [37] F. Ajzenberg-Selove, *Nucl. Phys. A* **300**, 1 (1978).
 [38] E. J. Evers, J. W. de Vries, G. A. P. Engelbertink and C. Van der Leun, *Nucl. Instrum. Methods Phys. Res., Sect. A* **257**, 91 (1987).
 [39] We disagree with Ref. [38] on the correct procedure for converting from a proton energy to energies for the ^{19}F beams. Our error includes this difference in beam energies.
 [40] J. F. Ziegler, *Stopping Cross-Sections For Energetic Ions In All Elements* (Pergamon Press, New York, 1980).
 [41] E. G. Myers, P. Kuske, H. J. Andrä, I. A. Armour, N. A. Jelley, H. A. Klein, J. D. Silver, and E. Träbert, *Phys. Rev. Lett.* **47**, 87 (1981); E. G. Myers, *Nucl. Instrum. Methods Phys. Res., Sect. B* **9**, 662 (1985).
 [42] We allow for the difference in the definition of the QED contribution as discussed in Ref. [10].